Light Switchable Bioorthogonal Reaction Manifold for Modulation of Hydrogel Properties

*Wai Lean Koay,[a] Gao Chang,[b] Quyen Vu Thi,[a] Xin Yi Oh,[a] Huihui Lin,[a] Saugat Mondal,[c] N. P. Pradeep Singh,[c] Xian Jun Loh,[d] Minh Thi Nguyet Le,[b] Vinh Xuan Truong[a, b,] *.*

[a]Institute of Sustainability for Chemicals, Energy and Environment (ISCE2), Agency for Science, Technology and Research (A*STAR), 1 Pesek Road, Jurong Island, Singapore, 627833, Republic of Singapore.

[b]Department of Pharmacology and Institute for Digital Medicine, Yong Loo Lin School of Medicine, National University of Singapore, Singapore, 117600, Republic of Singapore.

[c]Department of Chemistry, Indian Institute of Technology (IIT), Kharagpur, West Bengal 721302, India

[d]Institute of Materials Research and Engineering (IMRE), Agency for Science, Technology and Research (A*STAR), 2 Fusionopolis Way, Singapore, 138634, Republic of Singapore

KEYWORDS. Bioorthogonal ligation, hydrogels, photo-patterning, 3D cell culture, crosslinking, rheology.

Abstract

Chemical reaction systems that can occur via multiple pathways in controllable fashions are highly attractive for advanced materials applications and biological research. In this report, we introduce a bioorthogonal reaction manifold based on a chalcone pyrene (**CPyr**) moiety that can undergo either redshifted photoreversible [2+2] cycloaddition or thiol-Michael click addition. By coupling the **CPyr** to a water soluble poly(ethylene glycol) end-group, we demonstrate the efficient polymer dimerization and cleavage by blue light (λ = 450 nm) and UV light (λ = 340 nm), respectively. In the absence of light, the **CPyr** rapidly reacts with thiols in aqueous environments, enabling fast and efficient polymer end-group functionalization. The chemical reaction manifold was further employed in polymer crosslinking for the preparation of hydrogels whose stiffness and morphology can be modulated by different photonic fields, or addition of a thiol crosslinker. The photoreversible cycloaddition and thiol-Michael click addition can be used in conjunction for spatial and temporal conjugation of a streptavidin protein. Both crosslinking conditions are non-toxic to various cell lines, highlighting their potential in biomaterials applications.

Introduction

Controlling the outcome of a chemical reaction – especially when and where it can occur – is a critical factor for the successful development of its applications.[1-3] In the pursue of control over chemical reactivity, organic chemists have thus developed a plethora of chemical reaction systems with excellent chemo-selectivity as well as regioselectivity and/or stereoselectivity, enabling the construction of diverse molecular frameworks ranging from complex natural products to macromolecules and polymers. Contemporary research has further facilitated changes in the functions and properties by virtue of controlling the changes in molecular structures. Being able to manipulate chemical reactions in a spatial and/or temporal manner has indeed become essential

for many applications in e.g., tuning polymer architectures and networks,[4-7] additive manufacturing,[8-10] and surface modification.[11, 12] Specifically relating to biology research, functional designs composed of explicit chemical sequences are highly valuable for understanding, or even manipulating biological processes via localized drug delivery approaches, *in situ* bioconjugation and cell-labelling.[13-17]

Various click reactions have been introduced for (bio)materials engineering applications.[18-22] Many of these click reactions are thermally induced, often occurring spontaneously under physiological conditions, and thus control over the reaction onset is highly passive. Conversely, active control methods rely on an external stimulus to remotely initiate the reaction. Light is most commonly employed as the external stimulus to enable the precise spatial and temporal control.[23] More recently, both light- and thermal-initiated processes have been integrated into a single chemical reaction system to generate reaction manifold gated by light and partnering reactants. In particular, Lemieux *et al.* introduced a photoswitchable dithienylethene (DTE) system of which the open form isomer can undergo thermal Diels-Alder cycloaddition.[24] Based on such a DTE core, Branda and co-workers developed new polymer adhesives whose strength can be regulated via photo-induced locking and unlocking of the polymerization process.[25] The team of Hetch further developed several innovative applications in fine-tuning the self-healing of polymer films,[26] and remote-controlled capture and release of chemical reagents.[27] Applying the same concept, Kalow and co-workers utilized azobenzene boronic acids able to undergo either *cis*-/*trans*-photoisomerization or thermal exchange with diol compounds for dynamic tuning of hydrogel viscoelastic properties and photoreversible binding with biomacromolecules.[28] Hiltebrandt *et al.* introduced a light-controlled reaction manifold consisted of a *o*-quinodimethane species that can participate in both photo-induced Diels-Alder reaction or aldehyde-amine condensation.[29] Our

team in collaboration with the team of Barner-Kowollik reported the use of an azobenzene with redshifted photoisomerization, and only the *cis*- form can thermally react with a photogenerated ketene for two-color activated covalent bond formation.[30]

Within the toolbox of bioorthogonal photo-click reactions, [2+2] photocycloadditions are highly attractive as a photochemical reaction class for reversible transformation of (bio)materials properties under different irradiation of different wavelengths.[31-33] In this research space, our team has actively engineered the chemical structures of the aromatic substituents to introduced red-shifted [2+2] chromophores that can be activated by visible lights such as blue and green light.[34, 35] We further employ these systems in the construction of biocompatible hydrogel scaffolds whose stiffness can be remotely manipulated by visible light.[36] However, an unexplored aspect of these [2+2] chromophores is their reactivity towards thiols for the Michael click addition. Herein, we introduce a reaction manifold based on a chalcone pyrene (**CPyr**) chromophore of which the reaction pathway can be controlled by different photonic fields for photoreversible dimerization, or rapid thiol-Michael addition in aqueous environment (**Scheme 1**). We further demonstrate the fine-tuning of hydrogel stiffness and patterning of hydrogel substrate with a bioactive component, utilizing the manifold reactivity of the **CPyr** function. Furthermore, both the reaction pathways are shown to be non-toxic to cells, enabling the 3D encapsulation and culture of live cells without affecting their biological functions.

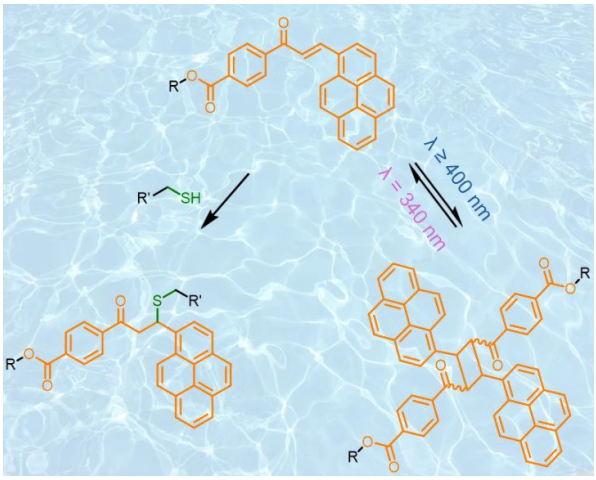

Scheme 1. A pyrene chalcone moiety that can undergo either thiol-Michael addition or redshifted [2+2] photocycloaddition in aqueous environment.

Experimental Methods

Materials

Chemicals and solvents for synthesis were purchased mainly from Sigma-Aldrich and TCI. 4-arm PEG_{20k}-OH was purchased from Jenkem Technology USA, Tetramethylrhodamine-labelled (TRITC) streptavidin was purchased from Thermo Fisher Scientific. Biotin-$PEG_{0.2k}$-SH was purchased from Biopharma PEG. All reagents were used as received.

Synthesis of Chalcone Pyrene (CPyr) Acid ((E)-4-(3-(pyren-1-yl)acryloyl)benzoic acid). Pyrene-1-carbaldehyde (2.3 g, 10 mmol) and 4-acetylbenzoic acid (1.64 g, 10 mmol) was dissolved in ethanol (20 mL). To this solution was added NaOH 10 M solution (5 mL) and the mixture was stirred at ambient temperature for 16 h. The mixture was neutralized to pH 6-7 using HCl 1M solution. The mixture was filtered and the solid was washed with excess water, dried in vacuo to give product as an orange solid (yield: 3.22 g, 85.64%). ^{1}H NMR (400 MHz, DMSO-d_6) 8.86 (d,

J = 15.3 Hz, 1H), 8.76 (d, J = 8.2 Hz, 1H), 8.54 (d, J = 9.4 Hz, 1H), 8.41 – 8.00 (m, 12H); ^{13}C NMR (100 MHz, DMSO-d6) 188.7, 166.8, 140.9, 140.3, 134.5, 132.6, 130.8, 130.1, 129.8, 129.7, 128.9, 128.8, 128.8, 127.9, 127.4, 126.6, 126.3, 126.0, 125.2, 124.9, 124.1, 123.8, 123.7, 122.2; HRMS (ESI) m/z: $[M+H]^+$ calcd for $C_{26}H_{17}O_3$, 377.1096 found 377.1167.

Synthesis of MeO-PEG-CPyr. MeO-PEG_{2k}-OH (2 g, 1 mmol) and chalcone pyrene acid (413 mg, 1.1 mol) were dissolved in DMF (10 mL). To this solution was added EDC.HCl (236.4 mg, 1.2 mmol) and DMAP (14.6 mg, 0.12 mmol) and the mixture was stirred at ambient temperature for 24 h. The solution was diluted with water (100 mL) and extracted with CH_2Cl_2 (50 mL x2). The combined organic phase was washed with brine (100 mL x2), dried ($MgSO_4$), and concentrated *in vacuo* to ca. 5 mL. The residue was added dropwise to diethyl ether (100 mL), and the polymer product was collected as off-white powder (yield: 1.67 g, 69.6%). ^{1}H NMR (400 MHz, Chloroform-d) 9.02 (d, J = 15.4 Hz, 1H), 8.55 (d, J = 9.3 Hz, 1H), 8.46 (d, J = 8.2 Hz, 1H), 8.28 – 8.13 (m, 9H), 8.13 – 8.03 (m, 2H), 7.81 (d, J = 15.3 Hz, 1H), 4.56 – 4.50 (m, 2H), 3.90 – 3.86 (m, 2H), 3.82 – 3.80 (m, 2H), 3.74 – 3.53 (m), 3.37 (s, 3H). **PEG_{20k}-(Cpyr)$_4$** was prepared from PEG_{20k}-$(OH)_4$ following a similar procedure, giving polymer product as white powder (yield: 76.2%).

Synthesis of MeO-$PEG_{0.2k}$-Thiol. Triethylene glycol monomethyl ether (1.6, 10 mmol), mercaptopropionic acid (2.18 g, 20 mL) and p-toluenesulfonic acid (10 mg, catalytic amount) were added to a solution of cyclohexane (100 mL). The mixture was heated at 100 °C under Dean-Stark condition for 8 h. Cyclohexane was evaporated in vacuo, and the residue was redissolved in dichloromethane (50 mL), washed with saturated $NaHCO_3$ solution (20 mL), water (20 mL), brine (20 mL), dried ($MgSO_4$), and concentrated in vacuo to give product as a clear oil (yield: 2.5 g, 67.7%). ^{1}H NMR (400 MHz, Chloroform-d) 4.18 – 4.09 (m, 2H), 3.63 – 3.56 (m, 2H), 3.56 – 3.49

(m, 6H), 3.46 – 3.39 (m, 2H), 3.25 (s, 3H), 2.72 – 2.60 (m, 2H), 2.60 – 2.52 (m, 2H); ^{13}C NMR (100 MHz, $CDCl_3$) 171.58, 71.95, 70.62, 70.59, 69.07, 63.78, 59.06, 38.44, 19.75. The NMR spectra in agreement with the previous report.[10]

PEG_{20k}-$(SH)_4$ was prepared from PEG_{20k}-$(OH)_4$ following a similar procedure, and the polymer was purified by precipitation in excess diethyl ether to give the product as a white powder (yield: 81.2%).

Light Sources for Irradiation. For investigation of photoreactivity of **CPyr** group, commercial LED lamps (15 W) with irradiance centered at 450 nm (**Figure S1**) were used and the intensity was calibrated at $I = 20$ mW·cm^{-2}. For photocycloreversion on NMR sample, a handheld RZXLED UV flashlight (1 W) with irradiance centered at 340 nm was used, and the intensity was calibrated at $I = 1$ mW·cm^{-2}. For photorheology investigation, an OmniCure s2000 UV curing lamp was used and the light emission was gated at 405 ± 2 nm ($I = 10$ mW·cm^{-2}) or 340 ± 2 nm ($I = 10$ mW·cm^{-2}) using appropriate optical bandpass filters.

Hydrogels Fabrication. Photocrosslinked hydrogels were prepared from an aqueous solution (10 wt%) of **PEG_{20k}-$(Cpyr)_4$** solution by irradiation with blue light (λ_{max} = 450 nm) using a 3W LED light, while hydrogel degradation was induced by irradiation with a handheld RZXLED UV flashlight (1 W) with irradiance centered at 340 nm and the intensity was calibrated at $I = 1$ mW·cm^{-2}. Spontaneously crosslinked hydrogels were prepared by mixing an aqueous solution (10 wt%) of **PEG_{20k}-$(Cpyr)_4$** and a solution (10 wt%) of **PEG_{20k}-$(SH)_4$** at equal volume ratio, or at different volume ratio with excess of **PEG_{20k}-$(Cpyr)_4$** for light induced manipulation of hydrogels properties.

Materials Characterization

Nuclear Magnetic Resonance Spectrometry (NMR). ^{1}H and ^{13}C NMR spectra were recorded on ECA 500 II spectrometer (400 MHz) or Bruker spectrometer (400 MHz) at ambient temperature. $CDCl_3$ or DMSO-d6 (Cambridge Isotope Laboratories, USA) were used as the solvents for the NMR analysis, and the chemical shift was calibrated using residual undeuterated solvents or tetramethylsilane (TMS) as the internal standard.

High resolution mass spectra (HRMS). HRMS were recorded on an Agilent 6210 Series 1969A ESI-TOF (time of flight) mass spectrometer using EI (electron ionization) or ESI (electrospray ionization). Liquid chromatography–mass spectrometry (LCMS) was recorded on an Agilent Single Quadrupole using atmospheric pressure ionization (API).

UV-Vis Spectroscopy. UV-Vis spectra were recorded on a PerkinElmer LAMBDA Series UV/Vis/NIR 950 spectrophotometer equipped with a photomultiplier detector. Samples were prepared in water or chloroform and measured in Hellma Analytics quartz high precision cells with a path length of 10 mm at ambient temperature.

Fluorescence Spectroscopy. Fluorescence spectra were recorded on an Agilent Cary Eclipse fluorescence spectrometer equipped with a Xenon flash lamp (80 Hz). The excitation wavelength was set to either 390 nm or 430 nm. Samples were prepared in water or chloroform and measured in Hellma Analytics quartz high precision cells with a path length of 10 mm at ambient temperature. **Rheological Measurements.** Rheological experiments were measured using an Anton Paar Physica 302M rheometer with a plate-plate configuration. The lower plate is made of quartz and the upper plate is made of stainless steel with a diameter of 25 mm. An OmniCure S2000 lamp was used as the light source, providing irradiation to underneath the quartz plate via

a cable light guide. The irradiation wavelengths were adjusted using bandpass filters at λ = 405 nm (I = 20 mW·cm^{-2}) or 340 nm (I = 10 mW·cm^{-2}). In a typical measurement, the polymer solution (100 μL) containing either **PEG$_{20k}$-(Cpyr)$_4$** or mixture of **PEG$_{20k}$-(Cpyr)$_4$** and **PEG$_{20k}$-(SH)$_4$** was placed on the quartz plate and the upper plate was brought down to a gap of 0.2 mm. The test was started by applying a 1% strain with a frequency of 0.1 Hz on the sample. After a period of 2-3 min, the LED light was switched on to initiate the photopolymerization.

Field Emission Scanning Electron Microscopy (FE-SEM) Measurements. Hydrogel morphology was studied with field emission scanning electron microscopy (FE-SEM) using JEOL JSM7900F. The freeze-dried hydrogel sample was placed on a clean silicon wafer attached to the sample stub, which was sputtered with gold. The accelerating voltage used was between 2 and 5 kV while the probe current was between 5 and 6 pA, depending on the sample.

Photopatterning of Hydrogel Substrate and Bioconjugation. Hydrogel was first fabricated by mixing a solution of **PEG$_{20k}$-(Cpyr)$_4$** (0.5 mL, 20 wt%) and **PEG$_{20k}$-(SH)$_4$** (0.5 mL, 10 wt%) and casted on a circular Teflon mold (diameter = 1.5 cm). The solution was left standing for 1 h at ambient temperature for thiol-Michael click crosslinking. Subsequently, the hydrogel was irradiated with blue light (450 nm) for 30 min to induce crosslinking via [2+2] photocycloaddition. The material was allowed to swell in excess DI water for 24 h and cover with a photomask. UV light (340 nm) was shone on top of the photomask for 30 min to induce cycloreversion. The photo-released **CPyr** group was then visualized using a fluorescence microscope EVOS M7000 (green channel). The hydrogel was then submerged in an aqueous solution containing biotin-PEG$_{0.2k}$-SH (2 μM) for 30 min and washed with excess DI water (3 times) over 3 h. The resultant hydrogel was then place in an aqueous solution of TRITC-streptavidin (0.1 mg·mL^{-1}) for 30 min, followed by washing with excess DI water and visualized using a fluorescence microscope (red channel).

Cell Encapsulation and Viability Assessment. To evaluate the potential cytotoxic effects of hydrogels under blue light irradiation on living cells, we conducted cell viability testing using three cell lines: human embryonic kidney (HEK-293T), Madin-Darby canine kidney (MDCK), and acute myeloid leukemia (MOLM13) cells. HEK-293T and MDCK cells were sourced from the American Type Culture Collection (ATCC, USA), while MOLM13 cells were obtained from the DSMZ Collection of Microorganisms and Cell Cultures (Germany). HEK-293T and MDCK cells were cultured in DMEM, and MOLM13 cells in RPMI 1640 (both from ThermoFisher Scientific, USA), each supplemented with 10% heat-inactivated FBS (Biosera, USA) and 1% penicillin/streptomycin (ThermoFisher Scientific, USA). All cell lines were maintained at 37°C with 5% CO2 in a humidified incubator.

We performed cell viability assays using the Cell Counting Kit-8 (CCK-8, MedChemExpress, USA) according to the manufacturer's instructions. Cells were seeded at 3x10^4 cells per well in 96-well plates and treated with 5% (w/v) Gel (i) or Gel (ii) for 24 hours. Post-treatment, 10 μL of CCK-8 reagent was added to each well and incubated for 1 hour at 37°C. Absorbance was measured at 450 nm using a Synergy H1 microplate reader (BioTek, USA), with wells without cells serving as blanks. Negative controls (DMEM or RPMI complete media) and positive controls (media with 20% DMSO) were included to validate the protocol. Data were analyzed using GraphPad Prism 10 (San Diego, CA, USA).

Results and Discussion

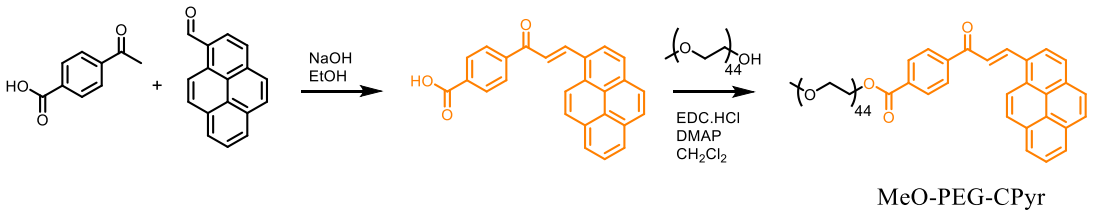

Scheme 2. Synthesis of chalcone pyrene acid via Claisen Schmidt condensation, which is subsequently used in Steglich esterification with MeO-PEG_{2k}-OH.

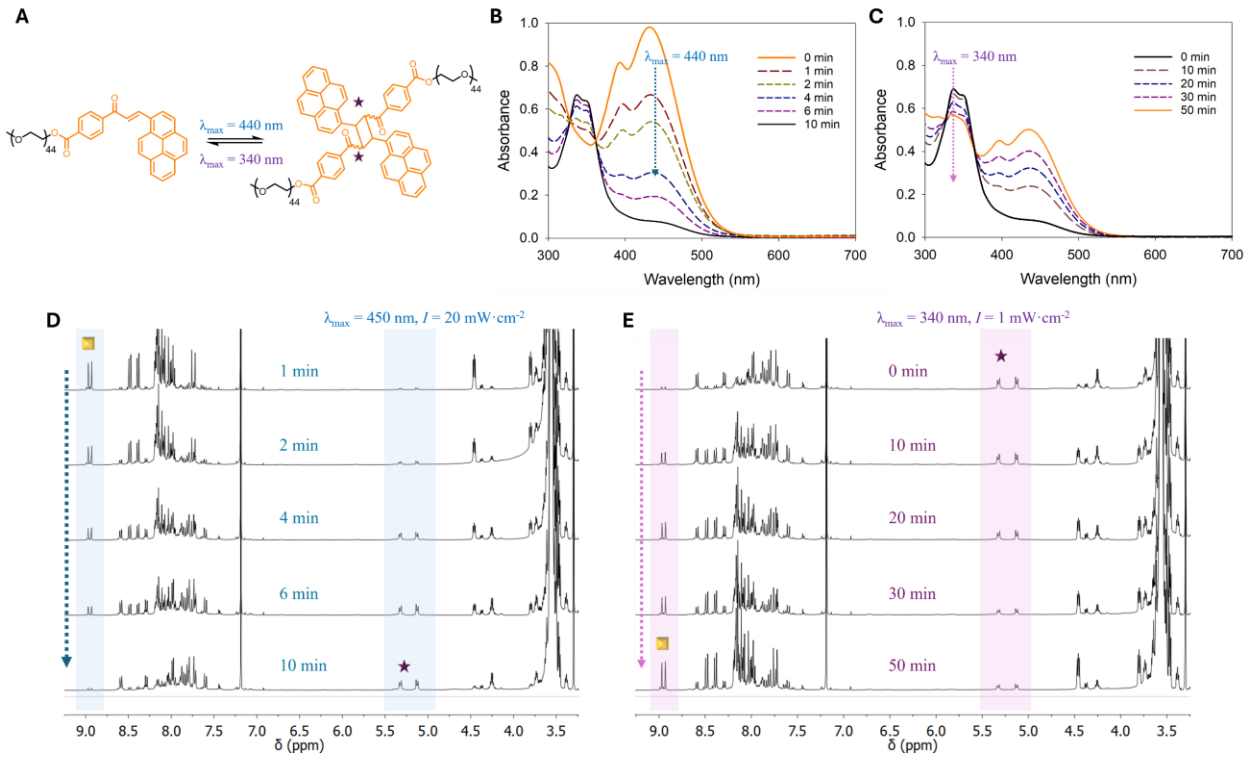

Figure 1. **A**) Scheme of reversible photodimerization of **MeO-PEG_{2k}-CPyr** by blue light and UV light, respectively. **B**) UV-Vis spectra of the **MeO-PEG_{2k}-CPyr** solution in water with increasing time of blue light irradiation, followed by **C**) UV light irradiation. **D**) ^{1}H NMR spectra of **MeO-PEG_{2k}-CPyr** (400 MHz, $CDCl_3$) products with increasing time of blue light irradiation, followed

by **E**) UV light irradiation; after each time interval, the solution was freeze-dried and redissolved in $CDCl_3$ for NMR measurement.

In our search for the bioorthogonal scaffold that display manifolds of reactivity, we examined the styrylpyrene moiety previously reported by our team for redshifted [2+2] photocycloaddition (**Figure S2**).[34] However, the styrylpyrene did not show any reactivity towards thiol even in the presence of base catalysts such as triethylamine (NEt_3) or in aqueous solution with pH = 9 (**Figure S2**). We thus examined the chalcone derivative that contains a pyrene substituent **CPyr** (**Scheme 2**), since chalcone moiety has been reported to have high reactivity towards protein thiols or reduced glutathione.[37, 38] The **CPyr** acid molecule can be readily synthesized from pyrene-1-carbaldehyde and 4-acetylbenzoic acid via Claisen-Schmidt condensation in good yield (>85%) and without the need for column chromatography purification. The acid was then coupled with a linear MeO-PEG-OH by Steglich esterification, giving a linear PEG polymer with **CPyr** endgroup, **MeO-PEG$_{2k}$-CPyr**, for investigation of the (photo)reactivity in water (**Figure 1A**). UV-Vis spectrum of aqueous solution of **MeO-PEG$_{2k}$-CPyr** shows a maximum absorbance at 432 nm (molar extinction coefficient ε = 78,000 $M^{-1}\cdot cm^{-1}$) and, and the absorbance extends to 520 nm. Therefore, we select a LED light source with the irradiance centered at λ_{max} = 450 nm (intensity I = 20 $mW\cdot cm^{-2}$) to initiate the photocycloaddtion. Upon exposure to such a blue light, the absorbance of **MeO-PEG$_{2k}$-CPyr** rapidly decreased, with a concomitance appearance of a blueshifted absorbance with an isosbestic point at 325 nm (**Figure 1B**) and 360 nm. Under UV light (λ_{max} = 340 nm, I = 1 $mW\cdot cm^{-2}$) irradiation the absorbance spectrum was reversed to the absorbance band corresponding to the **CPyr** absorbance (**Figure 1C**), indicating the photo-reversible dimerization of the **CPyr** moiety. It should be noted that pyrene based [2+2] chromophores have been reported to display redshifts in photoreactivity compared to their

absorption spectra, thus it may be possible to induce the photocycloaddition with green light ($\lambda \geq$ 510 nm). Together with the changes in UV-Vis absorbance of the polymer solution under light irradiation, we also observed the changes in fluorescence spectra. Specifically, there was a decrease in the intensity of the fluorescence band at 490 nm when the **CPyr** underwent photocycloaddition (**Figure S13**). This is due to the loss of the C=C bond and disruption of the conjugated structure. Following UV light irradiation, intensity of the fluorescence band at 490 nm also increased.

The light induced cycloaddition and cycloreversion processes were further confirmed by ^{1}H NMR spectroscopy. Under blue light irradiation, the chemical resonances of the alkene proton at 8.9 ppm rapidly decrease, followed by the concomitant increase of the resonances corresponding to the cyclobutane adduct at 5-5.5 ppm region (**Figure 1D**). When the dimer adduct was irradiated with UV light, we observed efficient cycloreversion, even at very low light intensity I = 1 mW·cm^{-2} (**Figure 1E**). These results strongly correlate to the UV-Vis study which shows the reversible photocycloaddition by blue light and UV light. Interestingly, when we investigated the photocycloaddition in deuterated chloroform, major *trans*-/*cis*- isomerization was observed (**Figure S10 and S11**) under identical irradiation conditions. The dominant photoisomerization under longer wavelength blue light (λ_{max} = 450 nm) in chloroform is in agreement with previous report by the team of Barner-Kowollik, which showed the major photo product of chalcone pyrene under irradiation of $\lambda \geq$ 440 nm is the *cis*- isomer.[39] Our study reveals that in addition to wavelength, solvent plays a significant role in dictating the outcome of the photoreactivity, since the major photoproduct observed in water is the cyclobutane adduct.

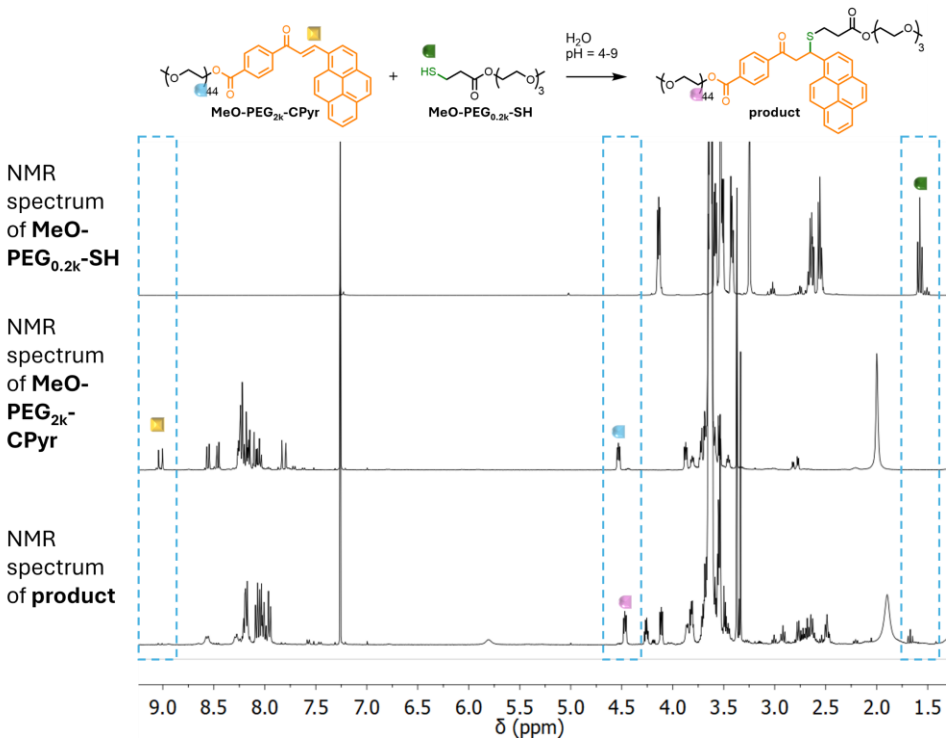

Figure 2. Scheme of the reaction between **MeO-PEG$_{2k}$-CPyr** and **MeO-PEG$_{0.2k}$-SH** in water at various pH values, and ^{1}H NMR spectra of the compounds (top) together with the spectrum of the product (bottom) showing near complete conversion after 15 min of reacting.

We next investigated the reactivity of **MeO-PEG$_{2k}$-CPyr** towards a water-soluble thiol **MeO-PEG$_{0.2k}$-SH**. Our initial investigation of the thiol-Michael addition was undertaken in DMSO using triethylamine (NEt_3) or tetramethylguanidine (TMG) as the base catalyst. In contrast to styrylpyrene, the **CPyr** displayed reactivity – as a Michael acceptor – towards thiol. However, the reaction rates were slow, with only 36% and 39% conversion in DMSO and catalyzed by triethylamine (10 mol%) and tetramethylguanidine (5 mol%), respectively after 8 h of reacting (**Figure S14** and **S15**). No reaction occurred in the absence of a base catalyst. Interestingly, when the reacting solvent was switched from DMSO to water, we observe complete conversion of the **CPyr** to thiol-addition adduct within 15 min and without the addition of any catalyst (**Figure 2**).

The reaction was found to be fast in water at different pH values ranging from 4 to 8, with complete conversion within 15 min of addition of **MeO-PEG$_{0.2k}$-SH**. Complete conversion was also observed in cell culture media within 15 min of reacting. The excellent reactivity of **CPyr** towards thiol in neutral and acidic conditions is interesting, since Michael reaction is typically base-catalyzed. The results thus suggest that neutral nucleophile RSH (Michael donor), instead of negatively charged RS^- is added to the **CPyr** moiety to form a zwitterion structure, followed by an intramolecular acid-base transfer to form the product (**Scheme 3**).[40] The thiol-Michael product is stable in water, however it slowly reversed to **CPyr** and **MeO-PEG$_{0.2k}$-SH** in DMSO, with *ca.* 34% conversion after 2 weeks (**Figure S15**). This result suggests that the Michael addition pathway of the **CPyr** moiety is dynamic by nature, and can be tuned by solvent switching.

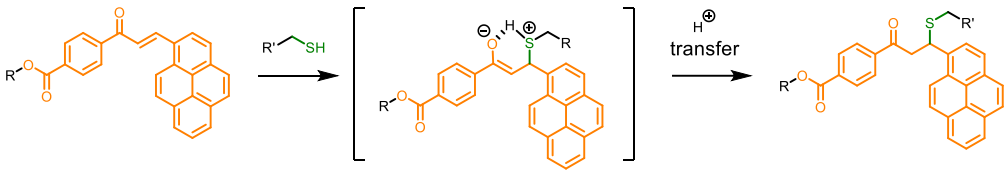

Scheme 3. Proposed mechanism of the nucleophilic addition to the activated double bonds of chalcone pyrene**.**

Having confirmed the manifold reactivity of the **CPyr** group, we next employed this function in hydrogel system for on-demand tuning of the materials properties in physiological conditions. Thus, we prepared 4-arm PEG (MW = 20,000 Da) having end group functionalized either with **CPyr** or thiol – henceforth referred to as **PEG$_{20k}$-(CPyr)$_4$** and **PEG$_{20k}$-(SH)$_4$**, respectively (**Figure 4A**). Subsequently, the polymer crosslinking in aqueous solution under different triggering conditions were investigated by rheology measurements. In the first test, we examined the hydrogel formation by mixing aqueous solutions of **PEG$_{20k}$-(CPyr)$_4$** (10 wt%) and **PEG$_{20k}$-(SH)$_4$**

(10 wt%) at equivalent volume ratio. As expected from the reactivity outcomes from linear polymers study, fast and spontaneous crosslinking via thiol-Michael click addition occurred upon mixing (**Figure 4B**), as indicated by the sharp increase in the storage modulus (G') value, reaching full gelation with a G' value of 3.8 kPa (Gel (**i**)) within 10 min. Furthermore, blue light (λ_{max} = 405 nm) and UV light (λ_{max} = 340 nm) did not cause any change in the G' value, suggesting that the **CPyr** group has been fully consumed. We then investigated the photo-crosslinking/decrosslinking of the **PEG_{20k}-$(CPyr)_4$**. Upon blue light (405 nm) exposure, the polymer rapidly crosslinked in solution (**Figure 4C**), reaching full gelation within 5 min giving a G' value of 1.7 kPa (Gel (**ii**)). The storage modulus of the hydrogel formed by light irradiation is noticeably smaller than that of the thiol-Michael click gel, which may be due to the rapid crosslinking and phase separation due to aggregation of the **Cpyr** groups, leading to less homogenous structure with lower mechanical strength. The crosslinked structure was fully decoupled under UV light (λ_{max} = 340 nm) irradiation, reaching the modulus of *ca.* 40 Pa within 3 min. The photo-crosslinking and photo-degradation of the same polymer solution can be repeatedly induced by alteration of blue and UV light irradiations. We noted that the G' value increase after each gelation/degradation cycle, which may be due to the secondary crosslinking from photooxidation under prolonged irradiation.

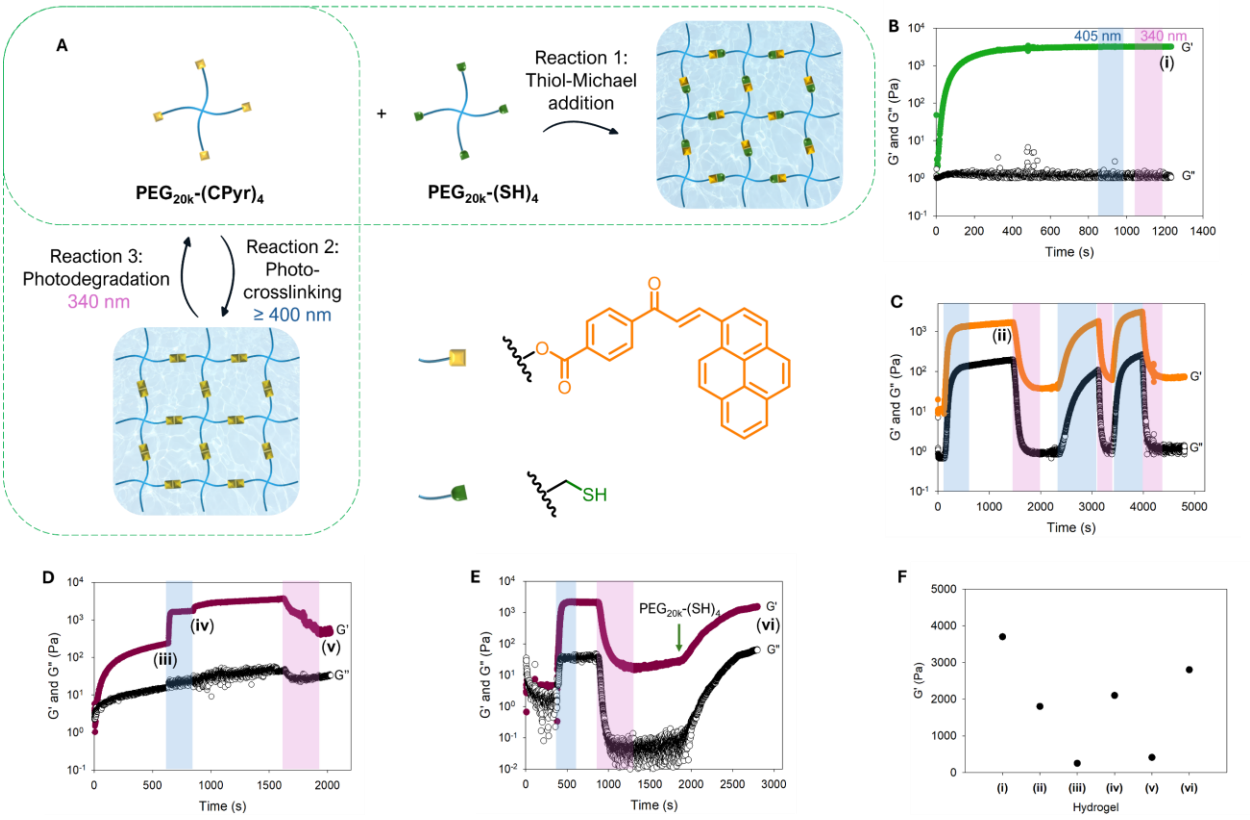

Figure 4. **A**) Schematic presentation of crosslinking via thiol-Michael addition (reaction 1), photo-crosslinking (reaction 2) and photodegradation (reaction 3) of 4-arm **PEG$_{20k}$-(CPyr)$_4$** by irradiation of blue light and UV light. Rheological assessment (time sweep) of **B**) spontaneous hydrogel formation by aqueous solutions of **PEG$_{20k}$-(CPyr)$_4$** (10 wt%) and **PEG$_{20k}$-(SH)$_4$** (10 wt%) at equivalent volume ratio; **C**) photo-crosslinking/decrosslinking of the **PEG$_{20k}$-(CPyr)$_4$** under irradiations of alternating blue light (λ = 405 nm) and UV light (λ_{max} = 340 nm) at the intensity of 10 mW·cm^{-2} from an Omnicure lamp; **D**) solution of **PEG$_{20k}$-(CPyr)$_4$** (10 wt%) and **PEG$_{20k}$-(SH)$_4$** (10 wt%) with excess of **PEG$_{20k}$-(CPyr)$_4$** volume ratio = 3:1, followed by treatment with blue light and UV light; **E**) photo-crosslinking/decrosslinking of the **PEG$_{20k}$-(CPyr)$_4$** solution by blue light and UV light, respectively, followed by addition of **PEG$_{20k}$-(CPyr)$_4$** (20 wt%). **F**)

Summary of the G' values obtained from hydrogels prepared under various crosslinking conditions described in Figures **4B**-**D**.

We further investigated the *in-situ* modulation of hydrogels' stiffness by varying the ratios of the reaction groups and the triggering conditions. Specifically, we employed a mixture of **PEG_{20k}-$(CPyr)_4$** and **PEG_{20k}-$(SH)_4$** with excess of **CPyr** compared to **SH** (**CPyr** : **SH** molar ratio = 2 : 1), keeping the polymer concentration at 10 wt%. The solution containing this polymer mixture formed hydrogels spontaneously upon mixing, with slower gelation kinetics (**Figure 4D**) and a lower G' (Gel (**iii**), ca. 0.28 kPa) value compared to the polymer solution containing equivalent molar ratio of **CPyr** to **SH**. After 5 min, the solution was subjected to blue light (405 nm) exposure, which leads to a sharp increase in G' value, reaching 2.1 kPa (Gel (**iv**)). Subsequently, the hydrogel formed by both thiol-Michael click addition and photocycloaddition was subjected to UV light irradiation, which resulted in the degradation of the network via cycloreversion, leaving the thiol-Michael crosslinked hydrogel (Gel (**v**)) with a G' value of 0.37 kPa. In another experiment, we first formed photo-crosslinked hydrogel by treatment of a **PEG_{20k}-$(CPyr)_4$** with blue light, followed by UV light-induced degradation of the network (**Figure 4E**). We then added **PEG_{20k}-$(SH)_4$** a – with equivalent molar ratio of **CPyr** and **SH** groups – to the residue and resume the rheology measurement. The resultant solution showed a spontaneous increase in the G' value, similar to pristine **PEG_{20k}-$(CPyr)_4$** and **PEG_{20k}-$(SH)_4$** mixture, reaching *ca.* 2.6 kPa (Gel (**vi**)) at complete gelation. This value is lower than the G' value of the pristine thiol-Michael addition network (3.8 kPa), and this result may be due to the uneven mixing of the **PEG_{20k}-$(SH)_4$**, forming a less heterogeneous network compared to the preparation for rheology measurement displayed in **Figure 4B**. The G' values of hydrogels formed in rheology experiments, Gels (**i**)-(**vi**) are summarized in **Figure 4F**, showing a range of moduli from 0.28 kPa to 3.8 kPa. Taking advantage

of the manifold reactivity of the **CPyr**, we have thus demonstrated the modulation of hydrogel stiffness by light and a thiol crosslinker. Such a control over stiffness can be valuable for the study of cell biology, especially in the area of mechanotransduction.

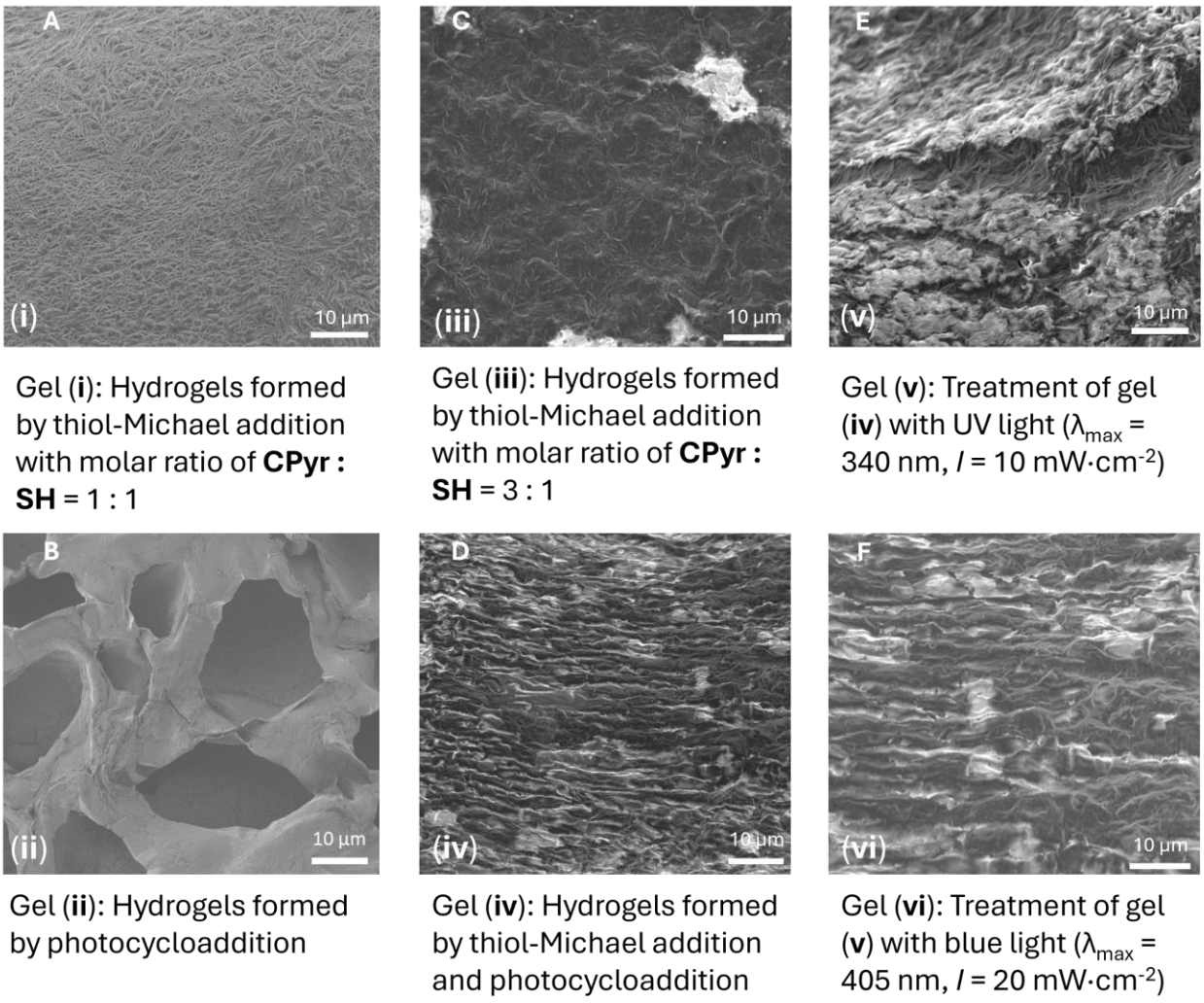

Figure 5. SEM images of hydrogels (**i**)-(**vi**) that were formed under various crosslinking conditions described in Figures **4B**-**D**.

We subsequently conducted SEM measurements to investigate the morphology of the hydrogels (**i**)-(**vi**) that were formed under different crosslinking conditions in the rheological assessment.

Interestingly, the thiol-Michael addition network showed a dense and interwoven fiber-like structure (**Figure 5A**, Gel (**i**)). In contrast, photocycloaddition network displayed a macro-porous structure with dense polymer phases, with pore size > 10 μm in diameter (**Figure 5B**, Gel (**ii**)). This difference in morphology clearly reflects the difference in the stiffness of the hydrogels, with Gel (**i**) possessing a higher G' value compared to Gel (**ii**) (3.8 kPa and 1.7 kPa, respectively). Gel (**iii**), with the molar ratio of **CPyr** : **SH** = 3 : 1, also displayed a fibrous structure with less dense polymer phase (**Figure 5C**) compared to Gel (**i**) (molar ratio **CPyr** : **SH** = 1 : 1). Gel (**iv**) that was formed by a combination of thiol-Michael addition and photocycloaddition showed a hybrid structure consisted of fibrous and laminar morphologies corresponding to the respective morphology observed in Gel (**i**) and Gel (**ii**). Under UV light (λ_{max} = 340 nm, I = 10 mW·cm^{-2}) irradiation, the laminar structure was observed to coagulate to large phases, while the fibrous morphology was retained (Gel (**v**), **Figure 5E**). Treatment of Gel (**v**) with blue light (λ_{max} = 405 nm, I = 20 mW·cm^{-2}) resulted in Gel (**vi**) with hybrid structure similar to the morphology observed in Gel (**iv**). The hydrogels' morphologies observed by SEM imaging have indeed matched with the moduli of the respective hydrogels, and thus demonstrated the tuning of hydrogel network structure using different irradiation conditions and/or input of a thiol crosslinker.

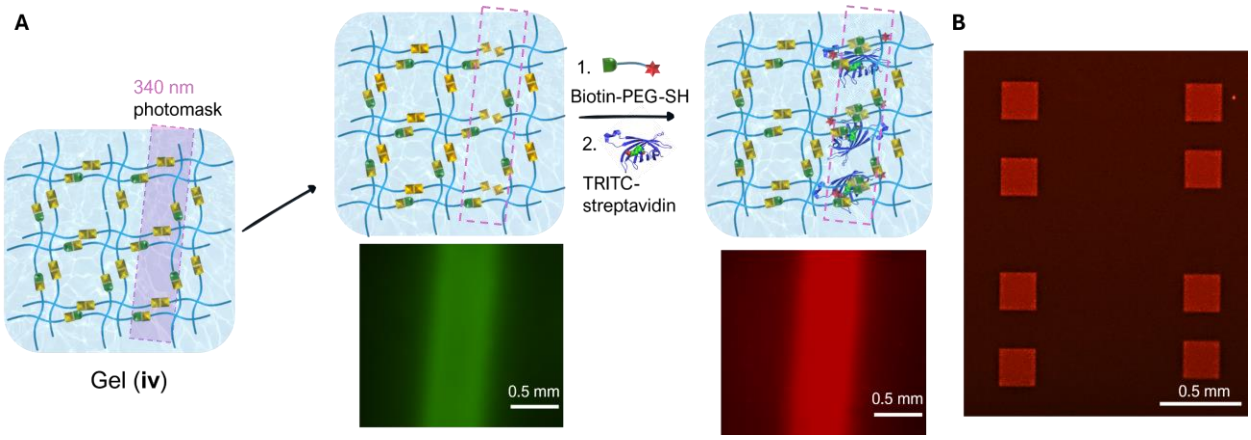

Figure 6. A) Schematic of patterning of hydrogel contained both photocycloaddition and thiol-Michael addition networks. The material was covered with a photomask and irradiated with UV light, where cycloreversion only occurred within the light-exposed region. The generation of the **CPyr** moiety can be observed using fluorescence microscope (bottom image, green channel). The **CPyr** can then react with a biotin-PEG-SH, followed by treatment with TRITC-streptavidin for bioconjugation via biotin streptavidin biding (red channel image). **B**) Square patterns of TRITC-streptavidin using the described light-induced cycloreversion patterning and thiol-Michael bioconjugation approach.

We further highlight the spatial and temporal control over hydrogels properties by patterning of the hydrogel with a bioactive reagent. Specifically, we selected Gel (**iv**) which contains both the Michael addition and photocycloaddition networks and irradiated the material with UV light (λ_{max} = 340 nm, I = 1 mW·cm^{-2}) for 10 min behind a photomask with specific patterns such as straight line and squares. The resultant hydrogel was then imaged under a fluorescence microscope. We observed the specific irradiated region that cycloreversion occurred (green channel), releasing the **CPyr** group that display green fluorescence (**Figure 6**). Subsequently, we treated the hydrogel with an aqueous solution of **biotin-PEG$_{0.2}$-SH** (2 μM), washed with DI water, and submerged the hydrogel in a solution of TRITC-streptavidin (0.1 mg·mL^{-1}) followed by thorough washing with DI water. The fluorescence image (red channel) of the resultant hydrogel indicated successful spatial conjugation of TRITC-streptavidin, via biotin streptavidin interaction, as shown by the red fluorescence region. This result indicates successful attachment of the biotin moiety to the patterned area via Michael addition onto the photoreleased **CPyr**.

To assess the suitability of both crosslinking pathways – photocycloaddition for Gel (**i**) and thiol-Michael click addition for Gel (**ii**) – in biomaterials application, we examined their effect on cell

viability by direct encapsulation of 3 cell lines: HEK-293T, MDCK, and MOLM-13 within the hydrogels. Specifically, cells were mixed with the polymer solutions and the crosslinking were induced by blue light irradiation, or mixing of the **PEG_{20k}-$(CPyr)_4$** and **PEG_{20k}-$(SH)_4$** (refer to **Figure 4B** and **4C** for preparation of Gel (**i**) and Gel (**ii**)). After 1 day of culture within the hydrogels, we did not detect any noticeable morphological changes in the cells under the microscope following treatment with either Gel (**i**) or Gel (**ii**) across all three cell lines. This visual assessment was supported by the results of the CCK-8 assay, which indicated that neither Gel (**i**) nor Gel (**ii**) caused cell death in any of the cell lines tested (**Figure 7**). Interestingly, both Gel (**i**) and Gel (**ii**) significantly increased the viability of MOLM-13 cells. We believe this effect may be due to the treatments stimulating cellular metabolic activity without necessarily increasing the number of cells. This enhanced metabolic activity could lead to greater reduction of the CCK-8 reagent, resulting in higher absorbance readings.

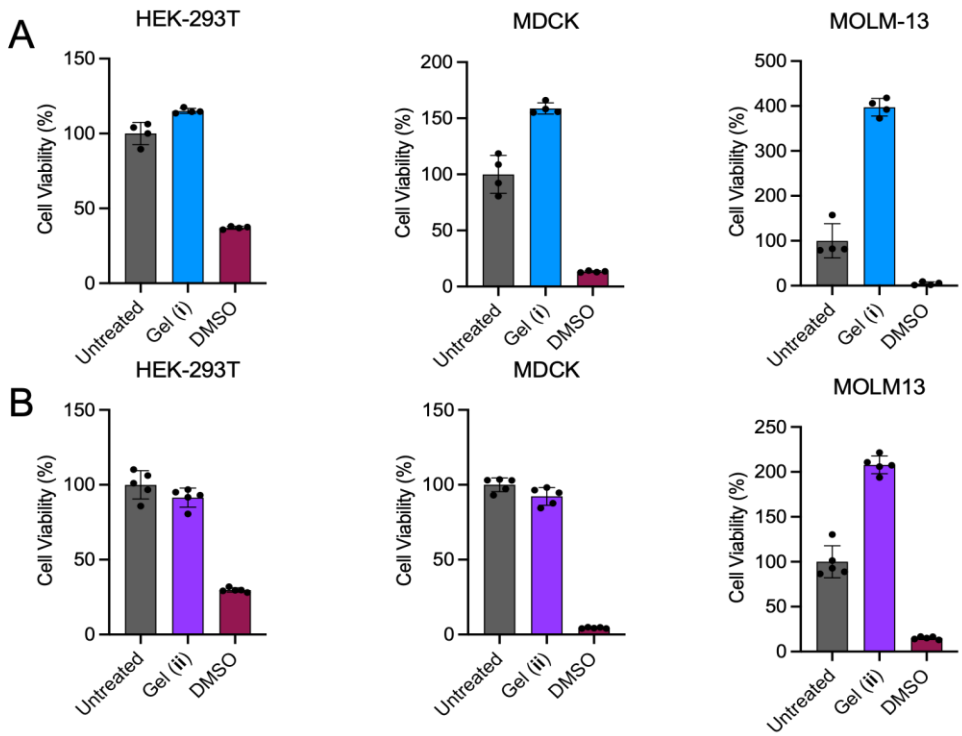

Figure 7. Assessment of viability of three cell lines HEK-293T, MDCK, and MOLM-13 encapsulated within the hydrogels via CCK-8 assay.

Conclusion

In conclusion, we report a chemical reaction manifold – based on a chalcone moiety with pyrene substituent on the alkenyl group – with two distinct reaction pathways: (i) reversible photocycloaddition by blue or UV light, or (ii) thiol-Michael click addition. We demonstrated the utility of such a reaction manifold in hydrogel formation and on-demand fine-tuning of the hydrogel's stiffness by changing the irradiation conditions or addition of a crosslinker. Furthermore, hydrogel materials can be readily photo-patterned with a bioactive reagent using a combination of reversible photocycloaddition and thiol-Michael click reaction. Critically, both reaction pathways are non-toxic to live cells, enabling the encapsulation and culture of cells within hydrogel network. Therefore, we submit that our chemical reaction manifold will find its use in (bio)materials engineering, as well as research on cell biology.

ASSOCIATED CONTENT

Supporting Information. The following files are available free of charge. Additional NMR data, fluorescence spectra of the compounds, irradiance spectra of the light source (file type, PDF).

AUTHOR INFORMATION

Corresponding Author

*Vinh X. Truong – Institute of Sustainability for Chemicals, Energy and Environment (ISCE2), Agency for Science, Technology and Research (A*STAR), 1 Pesek Road, Jurong Island, Singapore, 627833, Republic of Singapore; Email: vinh_truong@isce2.a-star.edu.sg

Author Contributions

The manuscript was written through contributions of all authors. All authors have given approval to the final version of the manuscript.

ACKNOWLEDGMENT

V.X.T. and M.T.N.L. acknowledge funding support from the Industry Alignment Fund – Pre-Positioning Programme (IAF-PP: H23J2a0130) for the development of new bioconjugation technologies. This research is additionally supported by the ASEAN-India S&T Development Fund (AISTDF) (File No- CRD/2022/000543).

ABBREVIATIONS

CPyr, chalcone pyrene; PEG, Poly(ethylene glycol); DTE, photoswitchable dithienylethene; NMR, nuclear magnetic resonance; HRMS, high resolution mass spectra; ESI-TOF, electron spray ionization – time of flight; LCMS, liquid chromatography–mass spectrometry; API, atmospheric pressure ionization; FE-SEM, field emission – scanning electron microscopy; NEt_3, triethylamine; TMG, tetramethylguanidine; UV-Vis, ultraviolet-visible; DMSO, dimethylsulfoxide; G', storage modulus; TRICT, Tetramethylrhodamine.

TABLE OF CONTENT GRAPHIC

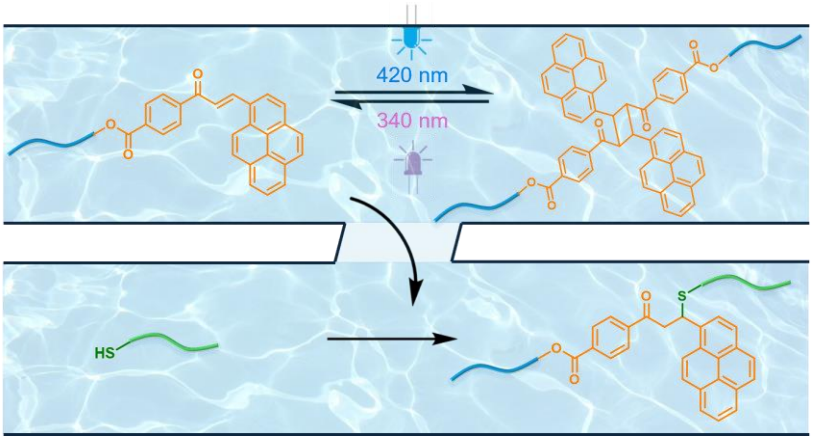

REFERENCES

1. Aubert, S.; Bezagu, M.; Spivey, A. C.; Arseniyadis, S., Spatial and temporal control of chemical processes. *Nature Reviews Chemistry* **2019,** *3* (12), 706-722.
2. McCune, J. A.; Mommer, S.; Parkins, C. C.; Scherman, O. A., Design Principles for Aqueous Interactive Materials: Lessons from Small Molecules and Stimuli-Responsive Systems. *Advanced Materials* **2020,** *32* (20), 1906890.
3. Irshadeen, I. M.; Walden, S. L.; Wegener, M.; Truong, V. X.; Frisch, H.; Blinco, J. P.; Barner-Kowollik, C., Action Plots in Action: In-Depth Insights into Photochemical Reactivity. *Journal of the American Chemical Society* **2021,** *143* (50), 21113-21126.
4. Kaupp, M.; Hiltebrandt, K.; Trouillet, V.; Mueller, P.; Quick, A. S.; Wegener, M.; Barner-Kowollik, C., Wavelength selective polymer network formation of end-functional star polymers. *Chemical Communications* **2016,** *52* (9), 1975-1978.
5. Kalayci, K.; Frisch, H.; Barner-Kowollik, C.; Truong, V. X., Wavelength-Dependent Stiffening of Hydrogel Matrices via Redshifted [2+2] Photocycloadditions. *Advanced Functional Materials* **2020,** *30* (15), 1908171.
6. Truong, V. X.; Barner-Kowollik, C., Photodynamic covalent bonds regulated by visible light for soft matter materials. *Trends in Chemistry* **2022,** *4* (4), 291-304.
7. Walden, S. L.; Nguyen, P. H. D.; Li, H.-K.; Liu, X.; Le, M. T. N.; Xian Jun, L.; Barner-Kowollik, C.; Truong, V. X., Visible light-induced switching of soft matter materials properties based on thioindigo photoswitches. *Nature Communications* **2023,** *14* (1), 8298.
8. Ehrmann, K.; Barner-Kowollik, C., Colorful 3D Printing: A Critical Feasibility Analysis of Multi-Wavelength Additive Manufacturing. *Journal of the American Chemical Society* **2023,** *145* (45), 24438-24446.
9. Zhang, X. N.; Zheng, Q.; Wu, Z. L., Recent advances in 3D printing of tough hydrogels: A review. *Composites Part B: Engineering* **2022,** *238*, 109895.
10. Gernhardt, M.; Truong, V. X.; Barner-Kowollik, C., Visible-Light-Degradable 3D Microstructures in Aqueous Environments. *Advanced Materials* **2022,** *34* (39), 2203474.
11. Heinz, O.; Aghajani, M.; Greenberg, A. R.; Ding, Y., Surface-patterning of polymeric membranes: fabrication and performance. *Current Opinion in Chemical Engineering* **2018,** *20*, 1-12.
12. Chen, W.-L.; Cordero, R.; Tran, H.; Ober, C. K., 50th Anniversary Perspective: Polymer Brushes: Novel Surfaces for Future Materials. *Macromolecules* **2017,** *50* (11), 4089-4113.

13. Shadish, J. A.; Benuska, G. M.; DeForest, C. A., Bioactive site-specifically modified proteins for 4D patterning of gel biomaterials. *Nature Materials* **2019,** *18* (9), 1005-1014.
14. Francis, R. M.; DeForest, C. A., 4D Biochemical Photocustomization of Hydrogel Scaffolds for Biomimetic Tissue Engineering. *Accounts of Materials Research* **2023,** *4* (8), 704-715.
15. Truong, V. X., Break Up to Make Up: Utilization of Photocleavable Groups in Biolabeling of Hydrogel Scaffolds. *ChemPhotoChem* **2020,** *4* (8), 564-570.
16. Li, M.; Dove, A. P.; Truong, V. X., Additive-Free Green Light-Induced Ligation Using BODIPY Triggers. *Angewandte Chemie International Edition* **2020,** *59* (6), 2284-2288.
17. Gulfam, M.; Sahle, F. F.; Lowe, T. L., Design strategies for chemical-stimuli-responsive programmable nanotherapeutics. *Drug Discovery Today* **2019,** *24* (1), 129-147.
18. Bird, R. E.; Lemmel, S. A.; Yu, X.; Zhou, Q. A., Bioorthogonal Chemistry and Its Applications. *Bioconjugate Chemistry* **2021,** *32* (12), 2457-2479.
19. Wu, D.; Yang, K.; Zhang, Z.; Feng, Y.; Rao, L.; Chen, X.; Yu, G., Metal-free bioorthogonal click chemistry in cancer theranostics. *Chemical Society Reviews* **2022,** *51* (4), 1336-1376.
20. Mitry, M. M. A.; Greco, F.; Osborn, H. M. I., In Vivo Applications of Bioorthogonal Reactions: Chemistry and Targeting Mechanisms. *Chemistry – A European Journal* **2023,** *29* (20), e202203942.
21. Yi, W.; Xiao, P.; Liu, X.; Zhao, Z.; Sun, X.; Wang, J.; Zhou, L.; Wang, G.; Cao, H.; Wang, D.; Li, Y., Recent advances in developing active targeting and multi-functional drug delivery systems via bioorthogonal chemistry. *Signal Transduction and Targeted Therapy* **2022,** *7* (1), 386.
22. McKay, Craig S.; Finn, M. G., Click Chemistry in Complex Mixtures: Bioorthogonal Bioconjugation. *Chemistry & Biology* **2014,** *21* (9), 1075-1101.
23. Fairbanks, B. D.; Macdougall, L. J.; Mavila, S.; Sinha, J.; Kirkpatrick, B. E.; Anseth, K. S.; Bowman, C. N., Photoclick Chemistry: A Bright Idea. *Chemical Reviews* **2021,** *121* (12), 6915-6990.
24. Lemieux, V.; Gauthier, S.; Branda, N. R., Selective and Sequential Photorelease Using Molecular Switches. *Angewandte Chemie International Edition* **2006,** *45* (41), 6820-6824.
25. Asadirad, A. M.; Boutault, S.; Erno, Z.; Branda, N. R., Controlling a Polymer Adhesive Using Light and a Molecular Switch. *Journal of the American Chemical Society* **2014,** *136* (8), 3024-3027.
26. Fuhrmann, A.; Göstl, R.; Wendt, R.; Kötteritzsch, J.; Hager, M. D.; Schubert, U. S.; Brademann-Jock, K.; Thünemann, A. F.; Nöchel, U.; Behl, M.; Hecht, S., Conditional repair by locally switching the thermal healing capability of dynamic covalent polymers with light. *Nature Communications* **2016,** *7* (1), 13623.
27. Göstl, R.; Hecht, S., Photoreversible Prodrugs and Protags: Switching the Release of Maleimides by Using Light under Physiological Conditions. *Chemistry – A European Journal* **2015,** *21* (11), 4422-4427.
28. Accardo, Joseph V.; Kalow, J. A., Reversibly tuning hydrogel stiffness through photocontrolled dynamic covalent crosslinks. *Chemical Science* **2018,** *9* (27), 5987-5993.
29. Hiltebrandt, K.; Elies, K.; D'hooge, D. R.; Blinco, J. P.; Barner-Kowollik, C., A Light-Activated Reaction Manifold. *Journal of the American Chemical Society* **2016,** *138* (22), 7048-7054.

30. Walden, S. L.; Rodrigues, L. L.; Alves, J.; Blinco, J. P.; Truong, V. X.; Barner-Kowollik, C., Two-colour light activated covalent bond formation. *Nature Communications* **2022,** *13* (1), 2943.
31. Truong, V. X.; Ehrmann, K.; Seifermann, M.; Levkin, P. A.; Barner-Kowollik, C., Wavelength Orthogonal Photodynamic Networks. *Chemistry – A European Journal* **2022,** *28* (25), e202104466.
32. Peng, T.; Dang-i, A. Y.; Liu, J.; Feng, C., [2 + 2] Photocycloaddition Reaction Regulated the Stability and Morphology of Hydrogels. *Advanced Fiber Materials* **2019,** *1* (3), 241-247.
33. Ping, X.; Pan, J.; Peng, X.; Yao, C.; Li, T.; Feng, H.; Qian, Z., Recent advances in photoresponsive fluorescent materials based on [2+2] photocycloaddition reactions. *Journal of Materials Chemistry C* **2023,** *11* (23), 7510-7525.
34. Truong, V. X.; Li, F.; Ercole, F.; Forsythe, J. S., Wavelength-Selective Coupling and Decoupling of Polymer Chains via Reversible [2 + 2] Photocycloaddition of Styrylpyrene for Construction of Cytocompatible Photodynamic Hydrogels. *ACS Macro Letters* **2018,** *7* (4), 464-469.
35. Kalayci, K.; Frisch, H.; Truong, V. X.; Barner-Kowollik, C., Green light triggered [2+2] cycloaddition of halochromic styrylquinoxaline—controlling photoreactivity by pH. *Nature Communications* **2020,** *11* (1), 4193.
36. Truong, V. X.; Bachmann, J.; Unterreiner, A.-N.; Blinco, J. P.; Barner-Kowollik, C., Wavelength-Orthogonal Stiffening of Hydrogel Networks with Visible Light. *Angewandte Chemie International Edition* **2022,** *61* (15), e202113076.
37. Rozmer, Z.; Perjési, P., Naturally occurring chalcones and their biological activities. *Phytochemistry Reviews* **2016,** *15* (1), 87-120.
38. Jin, Y. L.; Jin, X. Y.; Jin, F.; Sohn, D. H.; Kim, H. S., Structure activity relationship studies of anti-inflammatory TMMC derivatives: 4-Dimethylamino group on the B ring responsible for lowering the potency. *Archives of Pharmacal Research* **2008,** *31* (9), 1145-1152.
39. Carroll, J. A.; Pashley-Johnson, F.; Frisch, H.; Barner-Kowollik, C., Photochemical Action Plots Reveal Red-shifted Wavelength-dependent Photoproduct Distributions. *Chemistry – A European Journal* **2024,** *30* (23), e202304174.
40. Bernasconi, C. F., Nucleophilic addition to olefins. Kinetics and mechanism. *Tetrahedron* **1989,** *45* (13), 4017-4090.